

DECAY OF METASTABLE NONEQUILIBRIUM PHASES, ENHANCED REACTION RATE, AND DYNAMIC PHASE TRANSITION IN A MODEL OF CO OXIDATION WITH CO DESORPTION

Erik Machado and Gloria M. Buendía
*Physics Department, Universidad Simón Bolívar,
Apartado 89000, Caracas 1080, Venezuela*

Per Arne Rikvold
*Center for Materials Research and Technology,
School of Computational Science, and Department of Physics,
Florida State University, Tallahassee, Florida 32306-4052, USA
and Department of Fundamental Sciences, Faculty of Integrated Human Studies,
Kyoto University, Kyoto 606, Japan*

Robert M. Ziff
*Department of Chemical Engineering and
Michigan Center for Theoretical Physics,
University of Michigan, Ann Arbor, MI 48109-2136, USA*

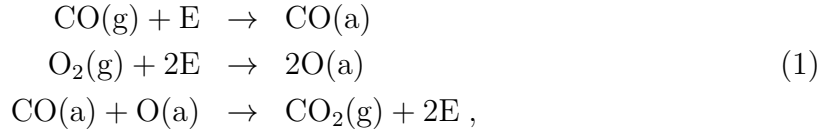
ABSTRACT

We present a computational study of the dynamic behavior of a Ziff-Gulari-Barshad model of CO oxidation with CO desorption on a catalytic surface. Our results provide further evidence that below a critical desorption rate the model exhibits a non-equilibrium, first-order phase transition between low and high CO coverage phases. Our kinetic Monte Carlo simulations indicate that the transition process between these phases follows a decay mechanism very similar to the one described by the classic Kolmogorov-Johnson-Mehl-Avrami theory of phase transformation by nucleation and growth. We measure the lifetimes of the metastable phases on each side of the transition line and find that they are strongly dependent on the direction of the transformation, i.e., from low to high coverage or vice versa. Inspired by this asymmetry, we introduce a square-wave periodic external forcing, whose two parameters can be tuned to enhance the catalytic activity. At CO desorption rates below the critical value, we find that this far-from-equilibrium system undergoes a dynamic phase transition between a CO₂ productive phase and a nonproductive one. In the space of the parameters of the periodic external forcing, this nonequilibrium phase transition defines a line of critical points. The maximum enhancement rate for the CO₂ production rate occurs near this critical line.

INTRODUCTION

The study of phase transitions and critical phenomena in nonequilibrium statistical systems have recently attracted a great deal of attention due its applications in many branches of physics, chemistry, biology, economics, and even sociology [1].

Within this field, surface reaction models have become an archetype for studying out-of-equilibrium critical phenomena, and they have been intensely analyzed with the purpose of designing more efficient catalytic processes [2]. The Ziff, Gulari, Barshad (ZGB) model [3] with desorption (the ZGB-k model) [4,5,6] describes kinetic aspects of the gas-phase reaction $\text{CO} + \text{O} \rightarrow \text{CO}_2$ on a catalytic surface in terms of two parameters: the relative partial pressure of CO, y , that represents the probability that the next molecule arriving to the surface is a CO, and the desorption rate, k , which is related to the probability that an adsorbed CO molecule is desorbed without being oxidized. The overall reaction is assumed to occur according to the Langmuir-Hinshelwood mechanism,



where E is an empty site on the surface, and (g) and (a) refer to the gas and adsorbed phase, respectively.

SIMULATIONS AND RESULTS

The ZGB-k model is simulated on a square lattice of linear size L that represents the catalytic surface. The kinetic Monte Carlo simulation generates a sequence of trials: CO or O_2 adsorption with probability $1 - k$, and CO desorption with probability k . For the adsorption, a CO or O_2 molecule is selected with probability y or $1 - y$, respectively. We calculate the coverages θ_{CO} and θ_{O} , defined as the fraction of surface sites occupied by CO and O, respectively, and the rate of production of CO_2 , R_{CO_2} . In Fig. 1 we show $P(\theta_{\text{CO}})$, the probability distribution for θ_{CO} vs y , where it is clearly seen that at a particular value of y , $y_2(k)$, a low θ_{CO} and a high θ_{O} phase coexist.

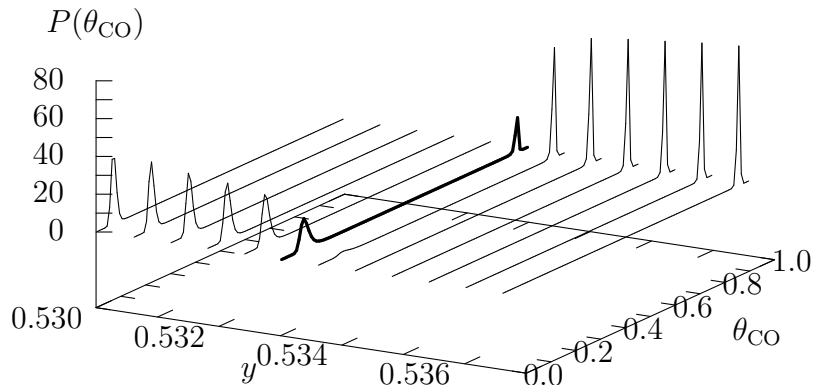


Figure 1: Order-parameter probability distribution, $P(\theta_{\text{CO}})$, for $k = 0.02$ and $L = 100$. The distribution for the value of y closest to the coexistence value, y_2 , is shown with a bold line.

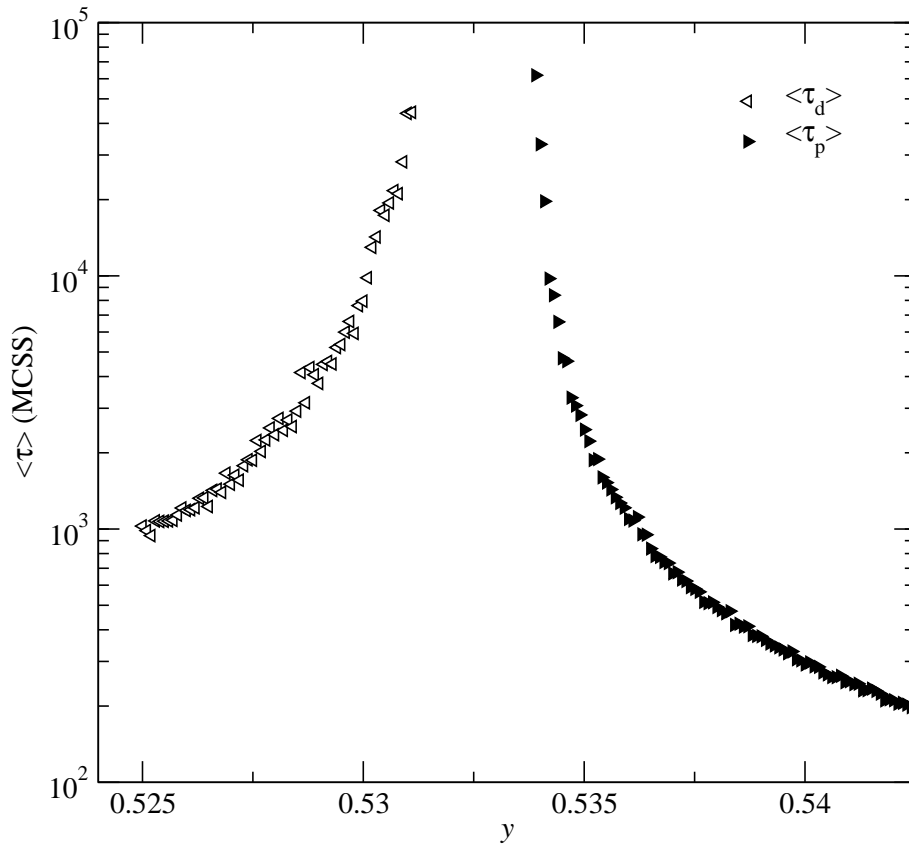


Figure 2: Decay times as functions of y when the system evolves toward the low CO coverage region $\langle \tau_d \rangle$, and when it evolves toward the high coverage region $\langle \tau_p \rangle$, shown for $k = 0.02$ and $L = 100$. Here and elsewhere in this paper, time is measured in Monte Carlo steps per site (MCSS).

A finite-size-scaling analysis of the statistical fluctuations of the CO coverage gives strong evidence that below the critical value of k the model exhibits a first-order, nonequilibrium phase transition between low and high CO coverage phases with the same characteristics as a first-order equilibrium phase transition [4,5,7].

We also measured the metastable lifetimes associated with the transition from the low CO coverage phase to the high CO coverage phase and vice versa. The system-size dependence of the decay times strongly suggests that the system follows a decay mechanism very similar to the one described by the classic Kolmogorov-Johnson-Mehl-Avrami theory of phase transformation by nucleation and growth near a first-order equilibrium phase transition, with well-defined single-droplet and multidroplet regimes [8,9]. In this system, the desorption parameter and the distance to the coexistence curve play the roles of the temperature and the supersaturation or overpotential, respectively. Near the coexistence curve the decay times are inversely proportional to $1/L$, and the decay mechanism consists of the nucleation and growth of a single droplet of the stable phase. Far from the coexistence curve, the decay times are independent of the system size, and the decay proceeds by random nucleation of many droplets of the stable phase [5].

We found that the lifetimes strongly depend on k and on the direction of the process; the mean decontamination time $\langle \tau_d \rangle$ (from high to low CO coverage) being

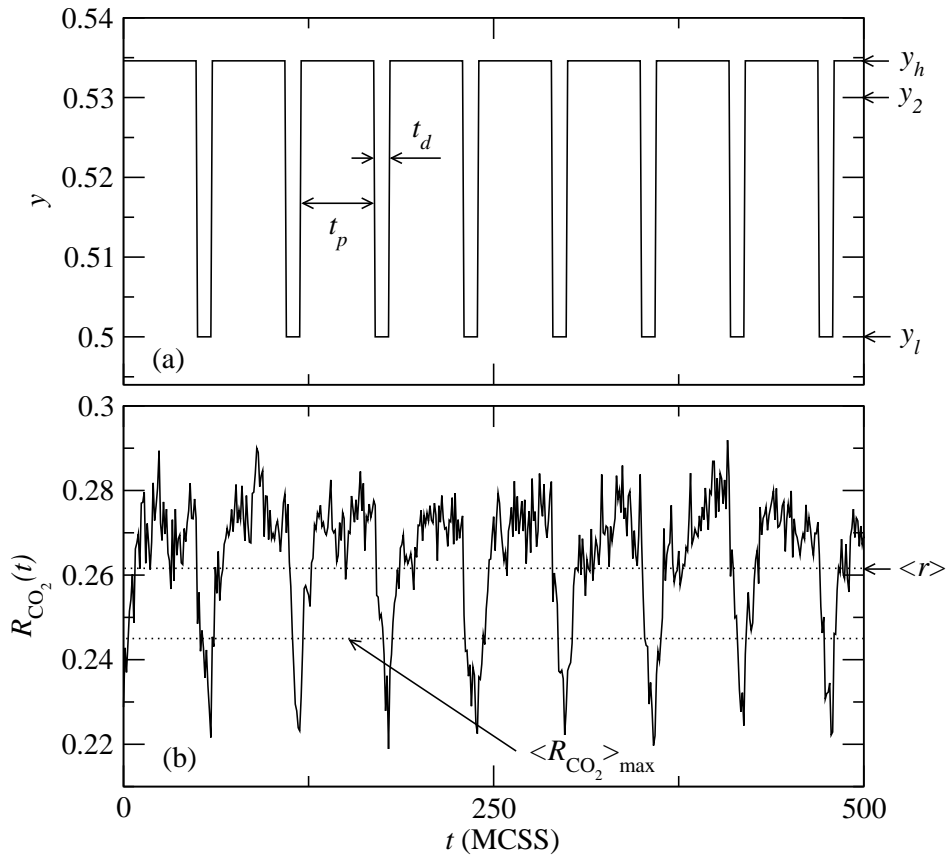


Figure 3: (a) Applied periodic pressure of CO, $y(t)$, that takes the values $y_l = 0.5$ and $y_h = 0.5346$ during the time intervals $t_d = 10$ and $t_p = 50$, respectively. (b) Response of the production rate to the applied pressure given in (a) for $L = 100$ with $k = 0.02$. The dotted line marked $\langle r \rangle$ indicates the long-time average of the period-averaged CO₂ production rate r , while the dotted line marked $\langle R_{\text{CO}_2} \rangle_{\text{max}}$ marks the maximum average CO₂ production rate for *constant* $y = y_2(k)$.

different from the mean poisoning time $\langle \tau_p \rangle$ (from high to low CO coverage). At comparable distances from the coexistence curve, $\langle \tau_d \rangle \gg \langle \tau_p \rangle$, as seen Fig. 2. Since several experiments indicate that it is possible to increase the efficiency of a catalytic process by subjecting the system to periodic forcing [10], we decided to exploit the asymmetry between the decay times by subjecting the system to a periodic variation of the external pressure with periods related to the decay times in each direction. We therefore select a square-wave periodic variation of the CO pressure, $y(t)$, that in a period $T = t_d + t_p$ takes the values, y_l (located below the transition pressure) during the time interval t_d and y_h (located above the transition pressure) during the time interval t_p , as can be seen in Fig. 3(a).

We found that the times that the driving force spends in the low and high coverage regions, t_d and t_p , respectively, can be tuned for each set of y_l and y_h to increase the productivity of the system. In Fig. 3(b) it is seen that the CO₂ production rate exhibits an oscillatory behavior in response to the periodic pressure shown in Fig. 3(a). The period-averaged value of the CO₂ production rate R_{CO_2} , defined as

$$r = \frac{1}{T} \oint R_{\text{CO}_2}(t) dt, \quad (2)$$

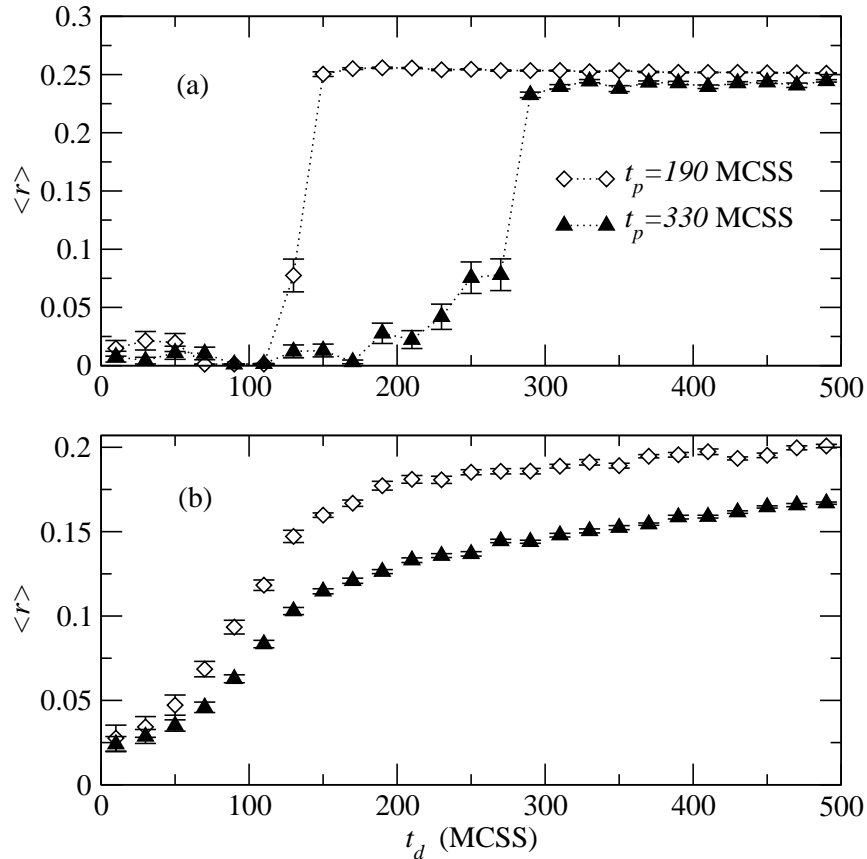


Figure 4: Long-time average of the period-averaged rate of CO₂ production, $\langle r \rangle$, shown vs t_d for two values of t_p and $L = 100$; (a) with $y_l = 0.52$, $y_h = 0.535$, and $k = 0.01$, and (b) with $y_l = 0.52$, $y_h = 0.553$, and $k = 0.04$. Only for the lower value of k does the system clearly present two dynamic phases: one with $\langle r \rangle \approx 0$ and the other with $\langle r \rangle > 0$.

plays the role of the dynamic order parameter [6]. For the parameters selected in Fig. 3, the long-time average of r , $\langle r \rangle$ takes a value that is about 7% higher than the maximum average CO₂ production rate for constant y . It is likely that more careful tuning of the parameters could further improve the degree of enhancement.

We also found that, for sufficiently low values of k , the driven system undergoes a dynamic phase transition between a dynamic phase of high CO₂ production, $r > 0$, and a nonproductive one, $r \approx 0$, as can be seen in Fig. 4. The distinction between these phases disappears for desorption rates above the critical value [6].

A detailed finite-size scaling analysis indicates that for small values of k , the measure of the fluctuations of the order parameter,

$$X_L = L^2[\langle r^2 \rangle - \langle r \rangle^2], \quad (3)$$

diverges as a power law with the system size, $X_L^{\max} \approx L^{\gamma/\nu}$ with exponent $\gamma/\nu = 1.77 \pm 0.02$, while moments of the order parameter at the transition point decay as $\langle r^n \rangle_L \approx L^{-n\beta/\nu}$ with $\beta/\nu = 0.12 \pm 0.04$. These exponent ratios, together with general symmetry arguments, give reasonable evidence that this far-from equilibrium phase transition belongs to the same universality class as the equilibrium Ising model [6].

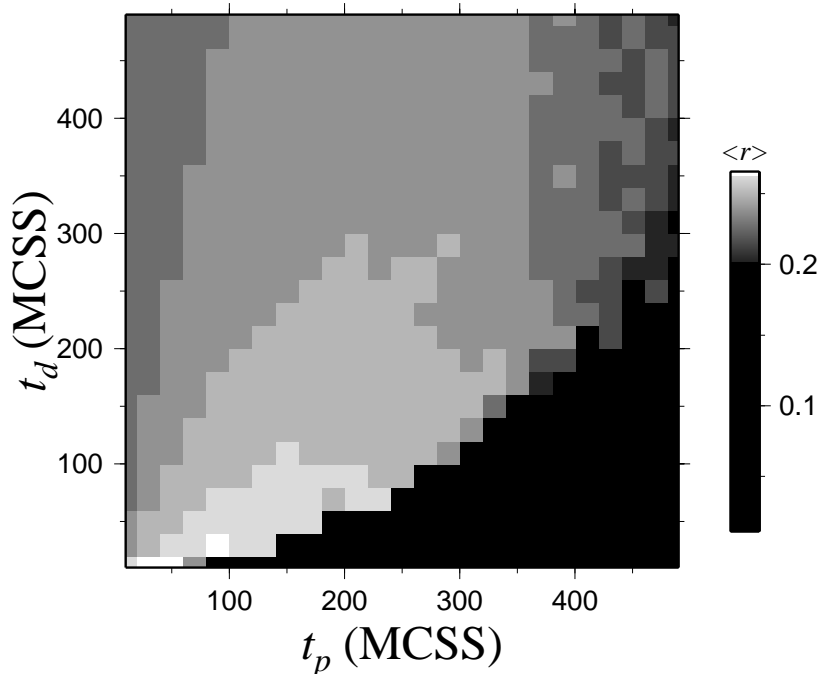


Figure 5: Long-time average $\langle r \rangle$ of the period-averaged CO₂ production rate r , shown as a density plot vs t_p and t_d for $y_l = 0.51$, $y_h = 0.535$, $k = 0.01$, and $L = 100$.

The long-time average production rate $\langle r \rangle$ is shown in a density plot vs t_p and t_d in Fig. 5. The line of critical points appears as the sharp boundary of the black, low-production region in the lower right-hand part of the figure. The region of maximum average production is seen to lie very close to the critical line on its high-production side. We believe this observation offers a clue to understanding the physical reason for the enhancement. Most likely, the long-range critical correlations associated with the critical cluster that develops for parameter values near the critical line produce a high density of sites where CO molecules would be situated next to O atoms, in positions conducive to rapid oxidation and desorption of the produced CO₂.

CONCLUSION

In this paper we have summarized results of large-scale kinetic Monte Carlo simulations of the ZGB-k model of heterogeneously catalyzed CO oxidation with CO desorption. The results of the simulations were analyzed using finite-size scaling methods. We found that there are strong similarities between the dynamics of metastable decay in this far-from equilibrium, non-Hamiltonian system and the well-known behavior of Hamiltonian systems. From a theoretical point of view, these similarities could lead to significant advancement in our understanding of the dynamics of far-from-equilibrium systems. From a practical point of view, our results can be exploited to develop novel ways to increase the efficiency of catalytic reactions.

ACKNOWLEDGMENTS

This work was supported in part by U.S. National Science Foundation Grant No. DMR-0240078 at Florida State University and Grant No. DMS-0244419 at The University of Michigan.

REFERENCES

1. H. J. Jensen, in *Self-Organized Criticality: Emergent Complex Behavior in Physical and Biological Systems*, Cambridge University Press, Cambridge (1998); J. Marro and R. Dickman, in *Non-equilibrium Phase Transitions in Lattice Models*, Cambridge University Press, Cambridge (1999)
2. K. Christmann, *Introduction to Surface Physical Chemistry*, Steinkopff Verlag, Darmstadt (1991); V. P. Zhdanov and B. Kazemo, Surf. Sci. Rep. **20**, 111 (1994); G. C. Bond *Catalysis: Principles and Applications*, Clarendon, Oxford (1987).
3. R. M. Ziff, E. Gulari, and Y. Barshad, Phys. Rev. Lett. **56**, 2553 (1986).
4. T. Tomé and R. Dickman, Phys. Rev. E **47**, 948 (1993).
5. E. Machado, G. M. Buendía, and P. A. Rikvold, Phys. Rev. E **71**, 031603 (2005).
6. E. Machado, G. M. Buendía, P. A. Rikvold, and R. M. Ziff, Phys. Rev. E **71**, 016120 (2005).
7. R. M. Ziff and B. J. Brosilow, Phys. Rev. A **46**, 4630 (1992).
8. A. N. Kolmogorov, Bull. Acad. Sci. USSR, Phys. Ser. **1**, 335 (1937); W. A. Johnson and R. F. Mehl, Trans. Am. Inst. Mining Metall. Eng. **135**, 416 (1939); M. Avrami, J. Chem. Phys. **7**, 1103 (1939); **8**, 212 (1940); **9**, 177 (1941).
9. P. A. Rikvold, H. Tomita, S. Miyashita, and S. W. Sides, Phys. Rev. E **49**, 5080 (1994).
10. R. Imbihl and G. Ertl, Chem. Rev. **95**, 697 (1995); M. Ehsasi, M. Matloch, O. Frank, J. H. Block, K. Christmann, F. S. Rys, and W. Hirschwald, J. Chem. Phys. **91**, 4949 (1989).